Anal. Chem. **2006,** *78,* 8339−8346

Surface Molecular Self-Assembly Strategy for TNT Imprinting of Polymer Nanowire/Nanotube Arrays

Chenggen Xie,[†,‡] Zhongping Zhang,[*,†,§] Dapeng Wang,[†] Guijian Guan,[†] Daming Gao,[†] and Jinhuai Liu[†]

Institute of Intelligent Machines, Chinese Academy of Sciences, Hefei, Anhui 230031, P. R. China, State Key Laboratories of Transducer Technology, Hefei, Anhui 230031, P. R. China, and School of Chemistry and Chemical Engineering, Anhui University, Hefei, Anhui 230039, P. R. China

This paper reports the finding of an investigation of a surface molecular self-assembly strategy for molecular imprinting of polymer nanowires/nanotubes. It has been demonstrated that 2,4,6-trinitrotoluene (TNT) templates were spontaneously assembled onto aminopropyl group-modified alumina pore walls by a strong charge-transfer complexing interaction between amino groups and electron-deficient nitroaromatics, forming a novel basis of surface molecular imprinting. While an additional amount of TNT templates was further replenished into a precursor mixture, a stepwise progressive polymerization was designed toward the controllable preparation of TNT-imprinted polymer nanowire/nanotube arrays in an alumina membrane. The imprinted nanowires/nanotubes with a high density of surface-imprinted sites and regular interior sites exhibit the high capacity of binding TNT molecules, which is nearly 2.5−3.0-fold that of normal imprinted particles. Moreover, the imprinted nanotubes and nanowires have ~6- and 4-fold increase in the rate of binding TNT molecules, respectively. The combination of surface molecular assembly with nanostructures in the imprinting technique can create more effective recognition sites than the only use of porogens in traditional approaches. This novel, facile strategy reported herein can be further expected to fabricate various molecular recognition nanoarrays for sensing or analytic applications.

The technique of molecular imprinting creates specific molecular recognition sites in solid materials by using template molecules. The most significant advantages of molecularly imprinted materials are mechanical/chemical stability, low cost, and ease of preparation and hence have attracted extensive research interest due to the potential applications in separation, sensors, bioassay, and drug delivery.[1−5]These attempts in applications generally emphasize that the imprinted materials are prepared in an optimizing form for obtaining high sensitivity, large binding capacity, and rapid binding kinetics.[2,6−10] Many imprinting strategies have recently been explored such as precipitation polymerization,[11] surface-graft coating,[12] monomolecular dendritic imprinting,[5] and surface molecular imprinting.[13−15] While various imprinted materials have been made, these efforts have met with only limited success in improving the molecular recognition properties.

Molecular imprinting typically involves the copolymerization of functional and cross-linking monomers in the presence of template molecules. Subsequent removal of template molecules from the polymer matrix generates the recognition sites (cavity) complementary to the shape, size, and functionality of the template. However, it is extremely difficult to extract the original templates located in the central area of the bulk/particular materials because the highly cross-linked rigid structure does not allow these molecules to move freely.[16] Furthermore, if the generated cavities are not in the proximity of the materials' surface, target species cannot still access the empty cavities encased within rigid matrix. As a result, traditional imprinting techniques most often produce the polymer materials exhibiting high selectivity but low binding capacity, poor site accessibility,

* To whom correspondence should be addressed. E-mail: zpzhang@iim.ac.cn.
† Institute of Intelligent Machines, Chinese Academy of Sciences.
‡ Anhui University.
§ State Key Laboratories of Transducer Technology.

(1) (a) Wulff, G. *Chem. Rev.* **2002**, *102*, 1. (b) Wulff, G. *Angew. Chem., Int. Ed.* **1995**, *34*, 1812. (c) Mosbach, K.; Ramström, O. *Bio/Technology* **1996**, *14*, 163. (d) Sellergren, B. *Molecularly Imprinted Polymers. Man-Made Mimics of Antibodies and their Application in Analytical Chemistry*; Elsevier: New York, 2001.
(2) Haupt, K.; Mosbach, K. *Chem. Rev.* **2000**, *100*, 2495.
(3) (a) Zimmerman, S. C.; Lemcoff, N. G. *Chem. Commun.* **2004**, 5. (b) Batra, D.; Shea, K. J. *Curr. Opin. Chem. Biol.* **2003**, *7*, 434.
(4) (a) Katz, A.; Davis, M. E. *Nature* **2000**, *403*, 286. (b) Bass, J. D.; Katz, A. *Chem. Mater.* **2003**, *15*, 2757.
(5) (a) Zimmerman, S. C.; Wendland, M. S.; Rakow, N. A.; Zharov, I.; Suslick, K. S. *Nature* **2002**, *418*, 399. (b) Mertz, E.; Zimmerman, S. C. *J. Am. Chem. Soc.* **2003**, *125*, 3424.
(6) Schmidt, R. H.; Mosbach, K.; Haupt, K. *Adv. Mater.* **2004**, *16*, 719.
(7) Shi, H.; Tsai, W.; Garrison, M. D.; Ferrari, S.; Ratner, B. D. *Nature* **1999**, *398*, 593.
(8) Yilmaz, E.; Haupt, K.; Mosbach, K. *Angew. Chem., Int. Ed.* **2000**, *39*, 2115.
(9) Hayden, O.; Mann, K. J.; Krassnig, S.; Dickert, F. L. *Angew. Chem., Int. Ed.* **2006**, *45*, 2626.
(10) Dai, S.; Burleigh, M. C.; Shin, Y.; Morrow, C. C. Barnes, C. E.; Xue, Z. *Angew. Chem., Int. Ed.* **1999**, *38*, 1235.
(11) Wang, J. P.; Cormack, A. G.; Sherrington, D. C.; Khoshdel, E. *Angew. Chem., Int. Ed.* **2003**, *42*, 5336.
(12) (a) Titirici, M. M.; Sellergren, B. *Chem. Mater.* **2006**, *18*, 1773. (b) Sellergren, B.; Rückert, B.; Hall, A. J. *Adv. Mater.* **2002**, *14*, 1204.
(13) Bossi, A.; Piletsky, S. A.; Piletska, E. V.; Righetti, P. G.; Turner, A. P. F. *Anal. Chem.* **2001**, *73*, 5281.
(14) Yang, H. H.; Zhang, S. Q.; Tan, F.; Zhuang, Z. X.; Wang, X. R. *J. Am. Chem. Soc.* **2005**, *127*, 1378.
(15) Li, Y.; Yang, H. H.; You, Q. H.; Zhuang, Z. X.; Wang, X. R. *Anal. Chem.* **2006**, *78*, 317.
(16) (a) Ki, C. D.; Oh, C.; Oh, S-G.; Chang, J. Y. *J. Am. Chem. Soc.* **2002**, *124*, 14838. (b) Markowitz, M. A.; Kust, P. R.; Deng, G.; Schoen, P. E.; Dordick, J. S.; Clerk, D. S.; Gaber, B. P. *Langmuir* **2000**, *16*, 1759. (c) Rao, M. S.; Dave, B. C. *J. Am. Chem. Soc.* **1998**, *120*, 13270.

10.1021/ac0615044 CCC: $33.50
Published on Web 11/15/2006

and slow binding kinetics. Thus, controlling template molecules to locate in the proximity of the materials surface is critical to creating more effective recognition sites and to improving site accessibility. Mosbach and co-workers developed a remarkably clever protocol for creating surface imprinting based on the covalent immobilization of template molecules on the surface of a solid substrate.[8] After polymerization and removal of substrate and templates, all recognition sites will only be situated at the surface of the imprinted materials. Unfortunately, the covalent linkage of template molecules on solid surfaces remains complicated and difficult/irreproducible, and the resulting products always have a low binding capacity because the total amount of recognition sites is very small.[13] Therefore, its application is limited.

As an alternative to these present approaches, molecular imprinting nanotechniques may provide a potential solution to these difficulties.[7,13−15,17,] Nanosized, imprinted materials are expected to possess several remarkable advantages over normal imprinting materials: (1) easy removal of template molecules because of extremely high surface-to-volume ratio; (2) higher binding capacity because of more recognition sites in the proximity of the surface; (3) faster binding kinetics due to easy accessibility to the target molecules; (4) well-defined morphology for feasible installation onto the surface of nanodevices. To date, however, molecularly imprinted nanostructured materials have been poorly explored in both preparation approaches and recognition properties. Our strategy is to develop the imprinted nanomaterials with high molecular recognition ability by combining nanostructures with surface imprinting, without using complicated chemical procedures.

Herein we report a surface molecular self-assembly strategy for molecular imprinting of polymer nanowire/nanotube arrays in porous alumina membrane. The explosive that has been of societal security concern, 2,4,6-trinitrotoluene (TNT), was used as a template compound. The imprinting strategy is based on the findings that TNT templates can spontaneously assemble onto 3-aminopropyltriethoxysilane (APTS)-modified alumina pore walls by a strong charge-transfer complexing interaction, instead of using chemical immobilization of template molecules on the surface. The assembly is very stable in the presence of functional monomers, ensuring that these assembled TNT templates are situated at the surface of imprinted nanostructures. In order to further enhance the total amount of recognition sites in the resulting imprinted nanostructures, an additional amount of TNT templates was replenished to the mixture solution of polymerization precursors. A stepwise progressive polymerization was rationally designed toward the controllable preparation of high-quality arrays of TNT-imprinted polymer nanowires and nanotubes. It has clearly been demonstrated that the binding capacities of imprinted nanowires and nanotubes to TNT molecules are 2.5−3.0-fold that of normal imprinted particles. Moreover, the imprinted nanowires and nanotubes have the nearly 4- and 6-fold increase in the rate of binding TNT molecules, respectively. Meanwhile, the TNT-imprinted nanostructures also show specific recognition selectivity for TNT molecules over related compounds such as 2,4-dinitrotoluene (DNT). The sensing nanoarrays could potentially be exploited for detecting the highly explosive and environmentally deleterious chemicals.

EXPERIMENTAL SECTION

Chemicals and Materials. The alumina membranes with pore diameters of ∼70 nm were prepared by electrochemical anodization, according to the reported method in the literature.[18] TNT and DNT were supplied by National Security Department of China and recrystallized with ethanol before use. APTS (Aldrich), ethylene glycol dimethacrylate (EGDMA; Aldrich), and analytical grade acetonitrile (Shanghai Chemicals Ltd.) were used as received. Azobisisobutyronitrile (AIBN) and acrylamide (Shanghai Chemicals Ltd.) were purified by recrystallized with ethanol and acetone, respectively.

Aminopropylsilane Modification of Alumina Pore Walls. Before modification, alumina membrane was cleaned in an ultrasonic bath using deionized water and ethanol and was then annealed (at 150 °C for 1 h) to expose the Al−O bonds on the pore wall surface.[19,20] Aminopropylsilane modification was carried out by a slightly modified method from that reported in the literature.[19−21] First, the annealed membrane was immersed into a mixture solution prepared by mixing 0.5 mL of 3-aminopropyltrimethoxysilane, 3 mL of ethanol, and 0.1 mL of sodium acetate buffer solution (pH 5.0). After a reaction period of 30 min, the membrane was taken out and rinsed with ethanol. Finally, silanization was accomplished by curing the membrane in an oven of 150 °C for 2 h under a nitrogen atmosphere.

TNT Self-Assembly on APTS-Modified Alumina Pore Walls. The APTS-modified alumina membrane was immersed into a 1 mM TNT solution (solvent: ethanol/acetonitrile, 8:2, v/v) for 6 h. The alumina membrane was taken out, washed with ethanol, and then dried under nitrogen flow at room temperature. TNT molecules were accordingly assembled onto the APTS-modified alumina membrane with a change from colorless to deep red.

Synthesis of TNT-Imprinted Nanowires and Nanotubes. TNT, acrylamide, EGDMA, and AIBN were dissolved in 30 mL of acetonitrile to make a mixture solution containing 0.02 M TNT, 0.08 M acrylamide, 0.48 M EGDMA, and 50 mg of AIBN. Several pieces of porous alumina membranes with TNT assembly on pore walls were immersed into the precursor solution in a glass tube. The mixture solution was degassed in an ultrasonic bath for 3 min and then purged with nitrogen for 10 min while being cooled in an ice bath. The reaction system was sealed under vacuum (∼1 mmHg) to ensure a full filling of the reaction solution in alumina membranes pores. The polymerization reaction was carried out in an oil bath by a three-step-temperature procedure. The reaction temperature was first elevated up to 40 °C for 2 h, then maintained at 53 °C for 6 h, and finally kept at 60 °C for 18 h. The products were further aged at 90 °C for 6 h to obtain high cross-linking density. The alumina membranes with TNT-

(17) Chronakis, I. S.; Milosevic, B.; Frenot, A.; Ye, L. *Macromolecules* **2006**, *39*, 357.

(18) Masuda, H.; Yamada, H.; Satoh, M.; Asoh, H. *Appl. Phy. Lett.* **1997**, *71*, 2770.

(19) Steinhart, M.; Wendorff, J. H.; Greiner, A.; Wehrspohn, R. B.; Nielsch, K.; Schilling, J.; Choi, J.; Gösele, U. *Science* **2002**, *296*, 1997.

(20) (a) Qiao, J.; Zhang, X.; Meng, X.; Zhou, S.; Wu, S.; Lee, S-T. *Nanotechnology* **2005**, *16*, 433. (b) Leger, C.; Lira, H. D. L.; Paterson, R. *J. Membr. Sci.* **1996**, *120*, 187.

(21) (a) Steinle, E. D.; Mitchell, D. T.; Wirtz, M.; Lee, S. B.; Young, V. Y.; Martin, C. R. *Anal. Chem.* **2002**, *74*, 2416. (b) Li, Y.; Yang, H. H.; You, Q. H.; Zhuang, Z. X.; Wang, X. R. *Anal. Chem*. **2006,** *78*, 317.

imprinted nanowires were mechanically polished to remove the polymer on the surface of the membrane. TNT-imprinted nanowires were obtained by removing alumina membranes with aqueous potassium hydroxide. TNT-imprinted nanotubes were synthesized by a slightly modified procedure: total concentration of polymerization monomers was reduced by 25%, and the initiator amount was increased from 50 to 80 mg. At the same time, nonimprinted nanowires/nanotubes were also synthesized according to the same procedure, and normal imprinted microparticles (2−3 μm in size) were produced in solution phase under identical chemical condition.

Measurements of Molecular Recognition Properties. Original TNT template molecules in the imprinted nanowires/nanotubes were extracted with a mixture solvent of CH_3OH/HAc (9 : 1, v/v) three times for 2 h each. The nanowires and nanotubes with imprinted sites were first suspended in a mixing ethanol/acetronitrile (8:2, v/v) solution with various TNT concentrations to make a mixture of 0.5 mg mL^{-1} nanowires or nanotubes. After incubation at room temperature for different time periods, the nanowires and nanotubes in the solution were removed by centrifugation. The bound amount of TNT in nanowires/nanotubes was determined by measuring the difference between total TNT amount and residual amount in solution with high-performance liquid chromatography. A slight change of concentration can be monitored by calculating the area of the chromatography peaks. Meanwhile, the binding kinetics was tested by detecting the temporal evolution of TNT concentration in the solutions. The recognition selectivity of the imprinted materials was investigated using the structure-analogous DNT as a compound competitive with TNT.

Characterizations. UV−visible absorbance spectra were measured with a UNIC UV-4802 spectrometer. The morphology of nanowires and nanotubes was examined by a FEI Sirion-200 field-emission scanning electron microscope (FE-SEM) and a JEOL 2010 transmission electron microscope. The infra spectra were recorded with a Nicolet Nexus-670 FT-IR spectrometer. The amount of TNT bound by nanowires/nanotubes was analyzed by means of a Waters Module-600 high-performance liquid chromatograph with UV 996 detector.

RESULTS AND DISCUSSION

The assembly of functional molecules on an organic monolayer by various noncovalent interactions has extensively been explored in the fabrication of biological and chemical sensors. In this work, we have developed a facile approach to assemble TNT template molecules onto the pore walls of the alumina membrane before imprinting synthesis was done. Alumina membrane was first modified with APTS, resulting in 3-aminopropyl monolayer on pore walls.[19−21] The assembly of TNT molecules on the pore wall is based on the very strong noncovalent interaction between the electron-deficient nitroaromatics and the electron-rich amino groups of APTS, which is analogous to the affinity binding of TNT molecules to an electron-rich semiconductive polymer.[22] The intermolecular interaction between TNT with APTS has been demonstrated by measurement of UV−visible absorbance spectra. Figure 1 shows the evolution of UV−visible spectra of TNT solution with increasing amount of APTS. Two new absorbing bands appear at 525 and 630 nm, respectively, and strengthen continuously with increasing APTS amount in the TNT solution, as indicated with the arrow in Figure 1. Meanwhile, we can see that the color of the mixture solution changes gradually from colorless to deep red. These suggest clearly the formation of a Meisenheimer complex between APTS and TNT in solution by the strong charge-transfer interaction.[23]

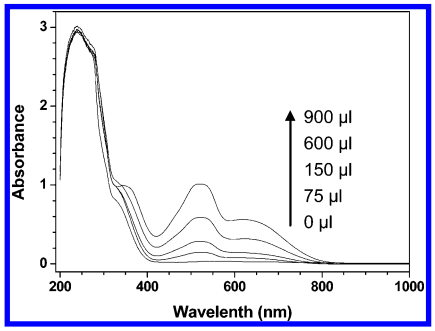

Figure 1. Evolution of UV−visible spectra with increasing APTS into 20 mL of 1 mM TNT solution (solvent: ethanol/acetonitrile, 8:2, v/v).

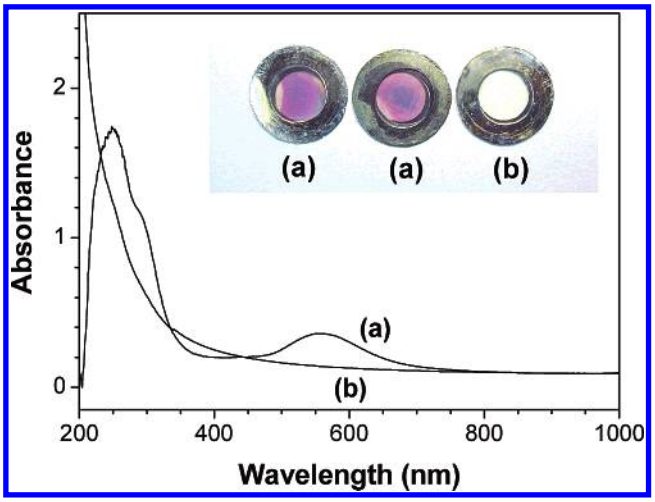

Figure 2. UV−visible spectra of TNT-assembled alumina membrane (a) and blank APTS-modified alumina membrane (b). Inset image shows the corresponding colors of APTS-modified alumina membranes after (a) and before (b) TNT assembly.

When APTS-modified alumina membranes are immersed into TNT solution, the strong complexing effects will accordingly drive TNT molecules to assemble on the alumina pore walls. The TNT assembly was carried out by simply immersing the APTS-modified alumina membrane into 1 mM TNT solution. The UV−visible spectra of alumina membrane in Figure 2 show that the TNT assembly on the 3-aminopropyl monolayer leads to a new visible band at 560 nm, in addition to the characteristic absorbance of TNT molecules at the ultraviolet region. Meanwhile, the color of APTS-modified alumina membranes changed rapidly into deep red from colorless, as shown in the inset image of Figure 2. These observations confirm clearly that TNT templates were assembled onto APTS-modified alumina pore walls by the charge-transfer complexing interaction in the solution system. Furthermore, because TNT is an electron-deficient Lewis acid, it may be that

(22) (a) Rose, A.; Zhu, Z.; Madigan, C. F.; Swager, T. M.; Bulovic, V. *Nature* **2005**, *434*, 876. (b) Yang, J. S.; Swager, T. M. *J. Am. Chem. Soc.* **1998**, *120*, 5321.

(23) Kang, S.; Green, J. P. *Proc. Natl. Acad. Sci. U.S.A.* **1970**, *67*, 62.

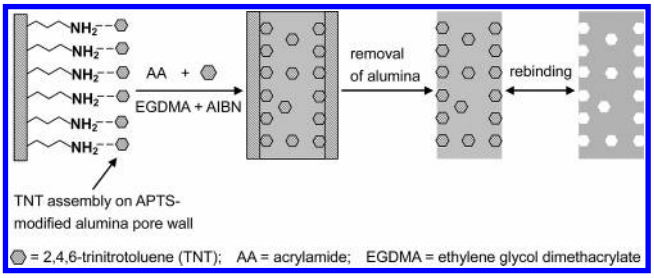

Figure 3. Schematic illustration of the TNT molecule assembly on APTS-modified alumina pore walls and the subsequent synthesis of TNT-imprinted nanowires with a high ratio of surface-imprinted sites.

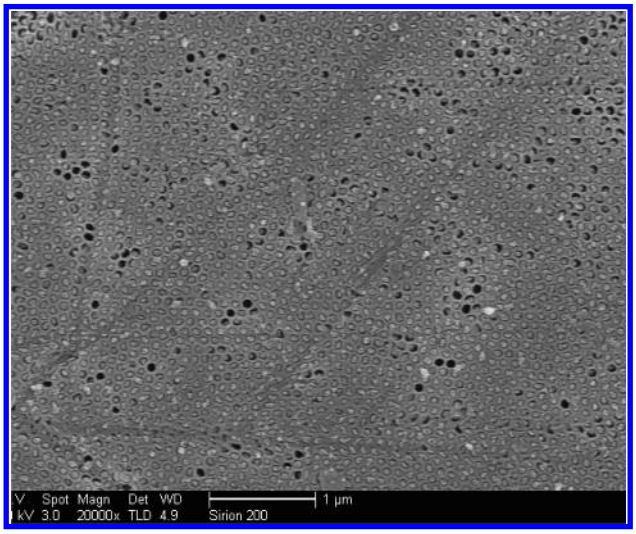

Figure 4. Top-view SEM image of the TNT-imprinted polymer nanowires embedded inside alumina membrane pores after membrane surface was mechanically polished.

the methyl group of TNT can be deprotonated by the amine groups (Lewis base) to form a TNT anion. The stronger interaction between TNT anions and amino cations will further strengthen the self-assembly of TNT templates on APTS-modified alumina pore walls. On the other hand, it was noted that the new visible absorbance (560 nm) resulting from TNT assembly has a shift of ~35 nm toward the long wave region, compared with the new absorbance (525 nm) in solution phase (Figure 1). The shift of absorbance band may suggest that TNT molecules were well oriented and densely arranged on the APTS monolayer.

Figure 3 illustrates the TNT molecular assembly on APTS-modified alumina pore walls and the subsequent synthesis of TNT-imprinted nanowires within alumina pores. Acrylamide was selected as the functional monomer for imprinting of the TNT molecules that assembled on the pore walls, because a relatively strong noncovalent interaction also lies between acrylamide and TNT molecules. The UV−visible spectrum reveals that adding acrylamide into TNT solution will produce two weak absorbances at 525 and 630 nm (data not shown). The color of the TNT solution changes from colorless into very slight red on adding acrylamide. However, the interaction between acrylamide and TNT is much weaker than the one between APTS and TNT because the acetyl amino group ($CONH_2$) is an electron donor much weaker than the alkane amino group (CH_2NH_2) of APTS. When we immersed the TNT-assembled alumina membranes into the polymerization precursor solution containing acrylamide, the deep red of alumina membranes did not fade. Therefore, the assembly of TNT molecules on the pore walls was very stable in the presence of functional monomers. This imprinting polymerization will be able to ensure that the assembled TNT templates locate at the surface of imprinted nanostructures, as shown in Figure 3. On the other hand, an additional amount of TNT was still replenished into the solution of polymerization precursors for to further create TNT recognition sites within nanowires by the noncovalent interaction between acrylamide and TNT molecules. For one-dimensional nanostructures with extremely high surface-to-volume ratio, these "regular" interior imprinted sites are still in the proximity of the surface and are thus effective for rebinding TNT molecules. The combination of surface molecular assembly with nanostructure was expected to produce a high ratio of surface-imprinted sites and to enhance the total amount of effective imprinted sites, as illustrated in Figure 3.

Typically, the in situ synthesis of TNT-imprinted nanowires in alumina membrane pores was carried out by simply immersing the TNT-assembled membranes (with a pore diameter of ~70 nm) into the mixture solution of polymerizing precursors and templates. Subsequent polymerization in a three-step-temperature procedure resulted in the growth of imprinted nanowires in template pores. Figure 4 shows a top-view SEM image of a piece of surface-polished alumina membrane. It can be clearly seen that a large-area array of polymer nanowires was embedded inside alumina membrane pores. Almost all membrane pores (more than 95%) were successfully filled with TNT-imprinted nanowires. The flat top surface suggests that the nanowire length is identical to the 100-μm thickness of the alumina membrane used. Highly oriented nanowire arrays can be obtained when the alumina membrane was partially dissolved with aqueous potassium hydroxide, as shown in Figure 5A. Furthermore, the nanowires can be liberated from template pores by complete removal of the alumina membrane. The SEM image of Figure 5B shows that the diameter of imprinted nanowires is ~70 nm and very uniform along its whole length.

Although the template fabrication in nanoporous alumina membranes is a common method in the production of nanowires and nanotubes, the in situ synthesis of imprinted polymer nanowires in the membrane pores is difficult under normal reaction conditions because the rapid precipitation of polymer always blocks the template channels of the alumina membrane at an early stage of polymerization. Here, we used a consecutive three-step-temperature procedure to achieve polymerization proceeding in a slow and progressive way. First, the precursor solution was heated at 40 °C for 2 h. At this early stage, the modified pore walls of the alumina membranes were easily wetted by the reaction solution. Then, the reaction temperature was elevated to 53 °C for 6 h. The prepolymerization of monomers took place at an extremely slow rate, and a small quantity of oligomers started to form and deposit onto the pore walls with the organic molecular layer, which is crucial to the successful synthesis of monodispersive nanowires. This process is very similar to the melt-wetting in the template fabrication of polymer nanotubes using melt polymers or oligomers.[19] Finally, the imprinted polymerization was completed at 60 °C for 18 h, and thus, the resulting polymer preferentially nucleated and grew on the TNT-assembled pore wall with polymer oligomers. This

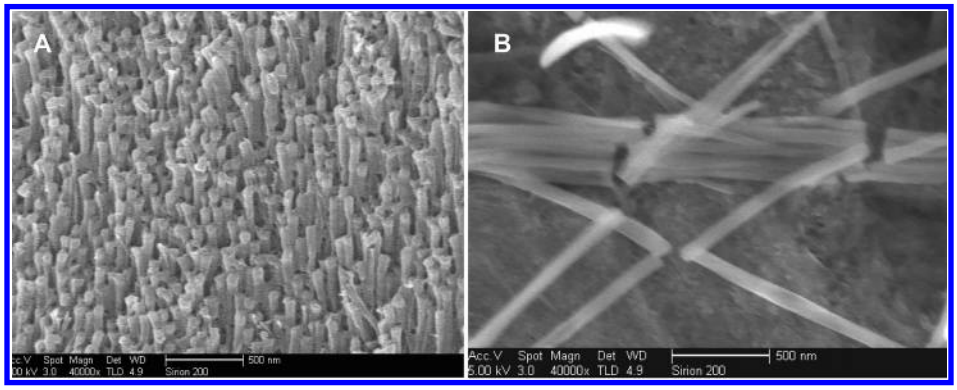

Figure 5. SEM investigation of TNT-imprinted polymer nanowires: (A) TNT-imprinted nanowire array obtained by partially dissolving alumina membrane and (B) individual nanowires liberated completely from alumina pores.

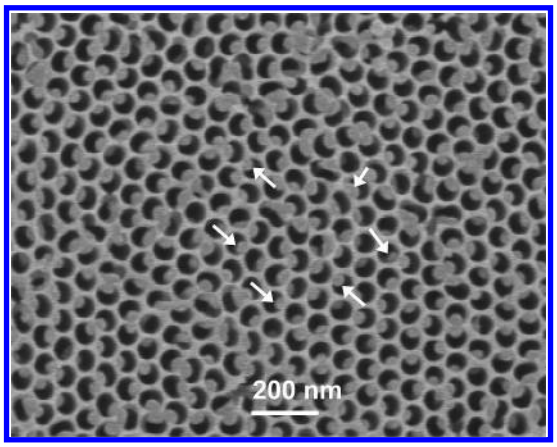

Figure 6. SEM observation on the intermediate growth stage of TNT-imprinted nanowires in alumina membrane pores.

stepwise procedure made the resulting polymer deposit along the pore walls but did not jam the alumina channels during polymerization. Figure 6 shows a top-view SEM image of alumina membrane after a reaction period of 6 h at 60 °C. As indicated with the arrows, we can clearly see that all nanowires were grown along one lateral side of the pore walls, leaving an obvious void between another lateral and the growing nanowires. Therefore, polymerization monomers can always diffuse into nanopores to continuously replenish the depletion of reaction nutrients. With increasing reaction period, finally, the alumina nanochannels will be closely filled up with imprinted nanowires, as shown in Figure 4. As a result, the assembled TNT templates on pore walls are entirely combined onto the surface of as-synthesized nanowires, and the well-developed morphology of the nanowire with a uniform diameter along its thorough length can be obtained (Figure 5B). At the same time, the additional TNT molecules in the reaction system were combined into the interior of nanowires. It should be noted that the nature of the cross-linker is another decisive factor for the in situ synthesis of uniform nanowires. As revealed by detailed experiments, when EGDMA without aromatic rings is used as a cross-linker to copolymerize with acrylamide, the resulting polymer or oligomer at an early stage may be solvated to a reasonable extent, and thus, the phase separation of polymer from solution is largely delayed.[24] The polymer precipitation will occur slowly along pore walls, which avoids jamming the channels of alumina.

(24) Coffey, D. C.; Ginger, D. S. *J. Am. Chem. Soc.* **2005**, *127*, 4564.

This synthetic approach also allows the production of TNT-imprinted nanotubes in alumina membrane pores by slightly modifying the reaction condition. When the total concentration of polymerization monomers was reduced by 25% and the initiator amount was increased from 50 to 80 mg, the amount of oligomer nucleating on the pore walls will be efficiently increased at an early stage because of the relatively rapid polymerization and longer phase separation time. A thin layer of surface film will cover the pore walls of the alumina membrane. The coverage of oligomers on the whole pore wall but not only along a lateral side can lead to the subsequent growth of nanotubes in template pores. The resulting nanotubes were closely embedded in the template pores, and the tips of nanotubes were clearly revealed by the SEM image of Figure 7A. The diameter of the nanotubes (~70 nm) corresponds well to the pore size of the alumina membrane used. Moreover, the ultra-thin-wall nanotubes with 10−15-nm wall thickness look almost transparent under the scanning electron microscopy, confirming that the nanotubes are hollow throughout their entire length, as shown in the inset of Figure 7A. The hollow structure of the nanotube was further examined with a transmission electron microscope (inset of Figure 7B). After etching the alumina membrane with aqueous potassium hydroxide, we can obtain a large-scale array of imprinted polymer nanotubes with monodispersive size and uniform orientation (Figure 7B). To our best acknowledge, the high-quality array of molecularly imprinted nanotubes was rarely reported in the previous research.

In this imprinting synthesis, TNT template molecules were sufficiently combined into nanowires/nanotubes by noncovalent interaction, which was confirmed by the FT-IR measurements as shown in Figure 8. Compared with the infra data of nonimprinted nanowires (Figure 8a), the imprinted nanowires displayed clearly the characteristic peaks of TNT molecules including the aromatic rings at 1548 cm^{-1} and nitro groups at 1350 cm^{-1} (Figure 8b). Moreover, the CH_3 peaks and the aromatic C−H stretches of TNT appear at ~2970 and ~3000−3100 cm^{-1}, respectively. However, these peaks are difficultly distinguished because they overlap with C−H stretch peaks of polymer nanowires. On the other hand, solvent extraction could provide an efficient removal of the TNT templates. These characteristic peaks of the TNT molecules disappeared completely after the extraction treatment (Figure 8c), and the IR spectrum became identical to that of the nonimprinted nanowires. This demonstrates that the surface molecular assembly strategy and the high surface-to-volume ratio of nanowires can

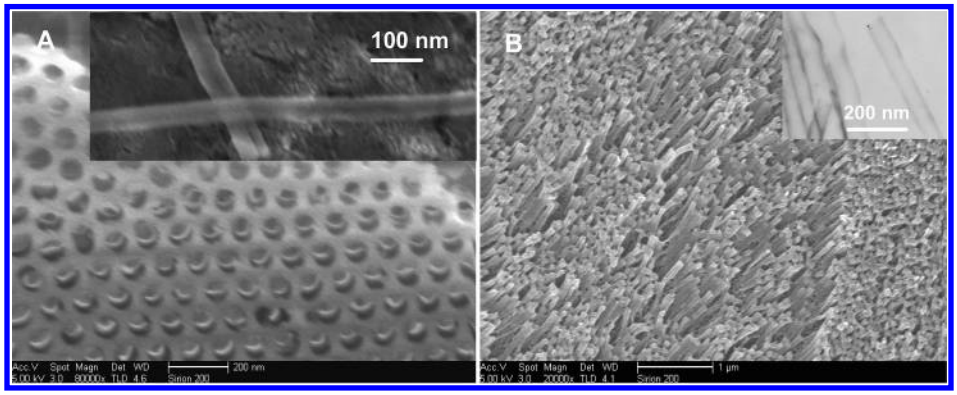

Figure 7. SEM observations of TNT-imprinted polymer nanotubes: (A) top-view SEM image of the nanotubes embedded inside alumina membrane pores (inset is high-magnification SEM image of single nanotubes) and (B) SEM image of the high-density array of nanotubes obtained by partially dissolving alumina membrane with aqueous potassium hydroxide (inset is the TEM image of the imprinted nanotubes).

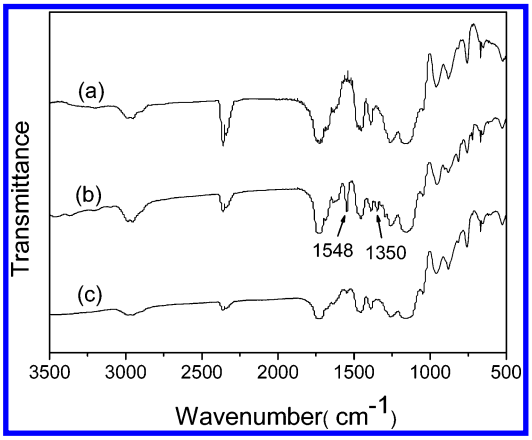

Figure 8. FT-IR spectra for (a) nonimprinted nanowires, (b) TNT-imprinted nanowires, and (c) TNT-removed imprinted nanowires.

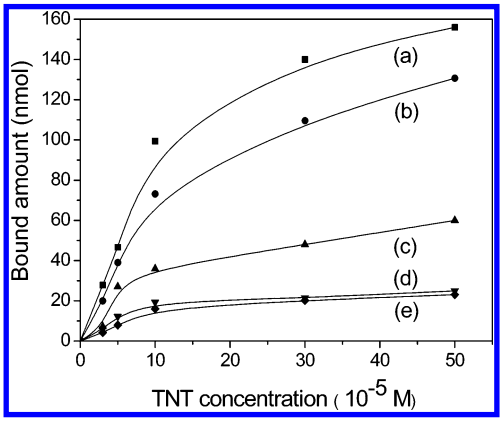

Figure 9. Amount of TNT molecules bound by imprinted nanotubes (a), imprinted nanowires (b), normal imprinted particles (c), nonimprinted nanotubes (d), and nonimprinted nanowires (e). All measurements were carried out by suspending 1 mg of imprinted materials in 2 mL of TNT solution.

simplify the removal of template molecules because most of the template molecules are situated at the surface or in proximity of surface.

The molecular recognition properties of the imprinted nanowires/nanotubes were evaluated by the measurement of their rebinding capacities to TNT molecules. As shown in Figure 9, the imprinting effect can be confirmed by the fact that imprinted nanowires and nanotubes show much higher binding capacities than nonimprinted ones. The maximum of rebinding capacities at equilibrium conditions are about 160 and 130 nmol mg^{-1} for the imprinted nanotubes and nanowires, respectively (Figure 9a, b). Moreover, the binding capacities are nearly 3- and 2.5-fold that of the normal imprinted particles with 2−3 μm in size (Figure 9c), respectively. The significant increase in binding capacity should be attributed to the high ratio of surface-imprinted sites, the large surface-to-volume ratios, and the complete removal of TNT templates. A greater number of effective imprinted sites are at the surface of materials or in the proximity of the surface for the one-dimensional imprinted nanostructures. Furthermore, Figure 9 also shows that the rebinding capacity of nanotubes is larger than that of nanowires, suggesting that a tubular nanostructure is the most favorable in improving the molecular imprinting effect. For the ultra-thin-wall nanotubes, the assay solution might easily diffuse down the length of the hollow core of the nanotube, and TNT molecules thus access these imprinted sites on the inside surface of nanotubes, which possibly increases the binding capacity of nanotubes to target molecules.

From the synthesis procedure used, there are two types of imprinted sites in the TNT-imprinted nanowires/nanotubes: the surface sites by surface self-assembly templates and the "regular" interior sites by addition of templates. Detailed experiments revealed that if the additional TNT templates had not been added to the synthesis system, the maximum of rebinding capacities by the surface-imprinted sites of nanotubes and nanowires are ~110 and ~85 nmol mg^{-1}, respectively. This suggests that the high binding capacities of nanotubes and nanowires are mainly contributed by surface-imprinted sites. Furthermore, it is possible to estimate the amount of surface-imprinted sites due to the uniform/regular morphology and size of nanowires and nanotubes. First, the surface area of nanowire can be calculated from the radius (r), weight (m), and density (ρ) of the polymer nanowire

$$S_{\text{wire}} = 2\pi rl = 2\pi r\left(\frac{m}{\rho}\frac{1}{\pi r^2}\right) = \frac{2m}{\rho\, r} \quad (1)$$

Similarly, the outer surface area of nanotube can be calculated from the outer radius (r_1), inner radius (r_2), weight (m), and density (ρ) of the polymer nanotube:

$$S_{\text{tube}} = 2\pi r_1 l = 2\pi r_1\left[\frac{m}{\rho}\frac{1}{\pi(r_1^2 - r_2^2)}\right] = \frac{2mr_1}{\rho(r_1^2 - r_2^2)} \quad (2)$$

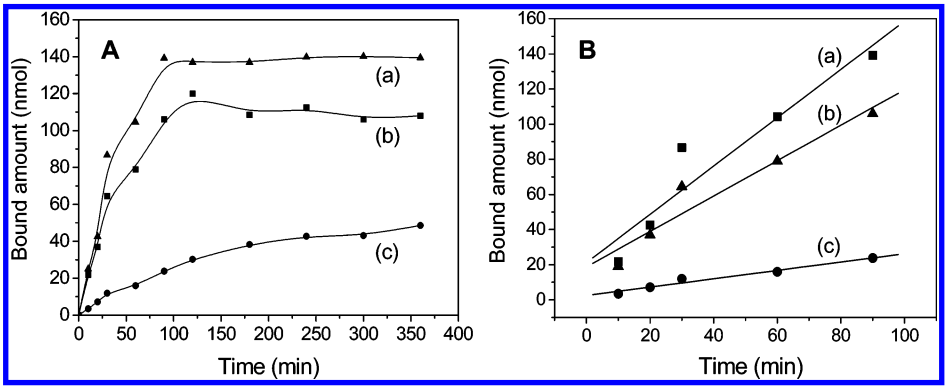

Figure 10. (A) Temporal evolution of the TNT amount bound by nanotubes (a), nanowires (b), and normal imprinted particles (c). (B) The fit lines of TNT binding kinetics of nanotubes (a), nanowires (b), and normal imprinted particles (c) before equilibrium adsorptions are reached. The points represent the mean values of three measurements obtained by suspending 1 mg of imprinted materials in 2 mL of 3.0×10^{-4} M TNT solution.

Then, the amount of surface-imprinted sites (q) on the imprinted nanowires and nanotubes can be estimated as

$$q_{\text{wire}} = \frac{S_{\text{wire}}\varphi}{\sigma_{\text{TNT}}N_{\text{A}}} = \frac{2m\varphi}{\sigma_{\text{TNT}}N_{\text{A}}\rho r} \quad (3)$$

$$q_{\text{tube}} = \frac{S_{\text{tube}}\varphi}{\sigma_{\text{TNT}}N_{\text{A}}} = \frac{2mr_1\varphi}{\sigma_{\text{TNT}}N_{\text{A}}\rho(r_1^2 - r_2^2)} \quad (4)$$

where φ, σ_{TNT}, and N_{A} represent the surface area percentage occupied by TNT monolayer, the size per TNT molecule, and the Avogadro constant, respectively. From the SEM and TEM observations in Figures 5 and 7, the imprinted nanowires/nanotubes have a uniform diameter of ~70 nm, and the inner diameter of the nanotubes is ~40 nm. Assuming a surface coverage percentage (φ) of 70%, a σ_{TNT} value of 8.0×10^{-15} cm^2, and a polymer density of 1 g cm^{-3}, the amount of surface-imprinted sites on the nanotubes and nanowires is estimated to be 123 and 84 nmol mg^{-1}, respectively. The calculation values are roughly in agreement with the experiment measurements on the binding capacities of the surface-imprinted sites of nanotubes and nanowires.

Figure 10A shows the temporal evolution of the amount of TNT bound by nanotubes, nanowires, and normal particles. Before equilibrium adsorption is reached, the imprinted nanotubes and nanowires can bind TNT molecules from solution phase at a much faster rate than normal imprinted particles. The imprinted nanotubes and nanowires took up 50% of the equilibrium adsorption amount during only ~25 and ~30 min and spent the equilibrium time periods shorter than ~90 and ~100 min, respectively (Figure 10A-a,b). Meanwhile, the normal imprinted particles needed ~110 min to take up 50% of the equilibrium adsorption amount, and the equilibrium period was longer than 300 min (Figure 10A-c). The fitting lines of binding kinetics are depicted in Figure 10B, revealing a rapid adsorption of TNT molecules into the imprinted nanotubes and nanowires. The binding rates obtained by the fitting results are 1.37, 1.01, and 0.24 nmol min^{-1} for imprinted nanotubes, nanowires, and normal particles, respectively. Therefore, the rebinding rates of imprinted nanotubes and nanowires to TNT molecules are about 6- and 4-fold that of the normal imprinted particles, respectively. The binding kinetics parameters are summarized in Table 1.

Table 1. Kinetics Parameters for the Imprinted Nanotubes, Nanowires, and Normal Particles[a]

	nanotube	nanowire	normal particle	$v_{\text{nanotube}}/v_{\text{normal particle}}$	$v_{\text{nanowire}}/v_{\text{normal particle}}$
v (nmol/min)	1.37 ± 0.22	1.01 ± 0.11	0.24 ± 0.01	6	4
$t_{1/2}$ (min)	25	30	110		
t_{equil} (min)	90	100	300		

[a] Binding rates (v) are obtained from the fit lines of binding kinetics in Figure 10B; $t_{1/2}$ represents the time for 50% of equilibrium adsorption amount. t_{equil} is the time for 100% of equilibrium adsorption amount.

From these above results, it is clear that the binding rates of TNT on the imprinted nanowires and nanotubes are remarkably faster than that on the normal imprinted particles. Usually, rapid binding kinetics requires that more recognition sites are at the surface or in the proximity of the surface for easy diffusion of target molecules into the recognition sites. Assuming a polymer density of 1 g cm^{-3} and a uniform diameter of 70 nm, the imprinted nanowires possess a specific surface area of ~571 cm^2 mg^{-1} by means of eq 1. Meanwhile, the surface area of normal microspheres with a 2-μm diameter is only ~30 cm^2 mg^{-1}. Therefore, in the normal imprinted particles with smaller specific surface area, most of the recognition sites locate in the interior of polymer matrix and are difficultly accessible to a target analyte, although porogens were used. In the nanowires or nanotubes, however, most of the recognition sites are at the surface or in the proximity of the surface due to their higher surface-to-volume ratio, which provide the higher site accessibility to the target analyte. The diffusional resistance to bring TNT into the recognition sites is thus much less than that of the normal imprinted particles. On the other hand, the thin nanowires/nanotubes are well dispersed throughout the assay solution, reducing further the mass-transfer resistance.[25]

The recognition selectivity of imprinted nanowires, nanotubes, and particles was measured using the structure-analogous DNT as a compound competitive with TNT. A partition coefficient (K)

(25) Hou, S.; Wang, J.; Martin, C. R. *Nano Lett.* **2005**, *5*, 231.

Table 2. Partition Coefficients and Selectivity Coefficients for TNT-Imprinted and Nonimprinted Materials ($n = 3$)

	partition coefficient (K)[a]						selectivity coefficient $\alpha = K_{Imp}/K_{Non-imp}$		
	TNT-imprinted			nonimprinted					
	nanotube	nanowire	normal particle	nanotube	nanowire	normal particle	nanotube	nanowire	normal particle
TNT	1399 ± 91	102 ± 63	592 ± 39	243 ± 17	222 ± 16	167 ± 13	5.76	4.61	3.54
DNT	301 ± 25	218 ± 19	170 ± 14	210 ± 14	163 ± 12	141 ± 11	1.43	1.34	1.21

[a] The solution concentration of TNT used to obtain the partition coefficients is 5.0×10^{-5} M.

can be calculated by the ratio of the bound amount of target molecule in imprinted materials and the residual amount in solution phase:[26]

$$K = \frac{\dfrac{\text{(moles of test compound bound to imprinted materials)}}{\text{(g of imprinted materials)}}}{\dfrac{\text{(moles of test compound remaining in solution)}}{\text{g of solution}}} \quad (5)$$

Furthermore, a comparison between the imprinted and nonimprinted materials was accomplished by calculating a ratio of the partition coefficients.

$$\text{selectivity coefficient } \alpha = K_{\text{Im p}}/K_{\text{Non-imp}} \quad (6)$$

The analyte concentration of 5×10^{-5} M was chosen to obtain the partition coefficient because it is in the linear part of the binding curve, as shown in Figure 9. For example, at the TNT concentration of 5×10^{-5} M, the bound amount of TNT molecules is ~39.0 μmol g^{-1}, while the residual amount in solution is ~38.1 nmol g^{-1}. Thus, the partition coefficient is estimated to be 1023 by eq 5. Table 2 lists the partition coefficients and selectivity coefficients for the imprinted and nonimprinted materials. From the data of the partition coefficient, all three imprinted materials have a greater uptake for TNT than for DNT. Meanwhile, the selectivity coefficient for TNT is much higher than that for DNT, indicating that the imprinted sites have a higher specificity for TNT than for DNT. In general, DNT should also be able to fit into the imprinted sites for TNT, but the binding affinity of the imprinted sites to DNT is much smaller than to TNT. This can roughly be understood from the imprinted procedure used. Due to the electron-drawn effect of nitro groups in nitroaromatics, a TNT molecule with three nitro groups is a stronger Lewis acid than DNT with two nitro groups. TNT molecules have a stronger interaction with a functional monomer (acrylamide, Lewis base) than DNT molecules. In other words, DNT will require a slightly stronger Lewis base as the imprinting functional monomer. Thus, the synthesized TNT-imprinted sites should have a higher binding affinity to TNT target molecules than to DNT. Comparing the K value of different nonimprinted materials in Table 2, we can see that nonimprinted materials have still a slightly larger affinity to TNT than to DNT. This further suggests a stronger interaction between functional monomer and TNT.

(26) Graham, A. L.; Carlson, C. A.; Edmiston, P. L. *Anal. Chem.* **2002**, *74*, 458.

CONCLUSIONS

We have demonstrated that electron-deficient nitroaromatics can spontaneously assemble on APTS-modified alumina pore walls, forming the novel basis of synthesizing surface molecularly imprinted materials without use of complicated chemical immobilization of template molecules. The surface molecular assembly strategy has been shown to be successful in creating the imprinted materials with a high ratio of surface-imprinted sites. Meanwhile, high-quality TNT-imprinted nanowire/nanotube arrays have been reproducibly produced in a controlled way. The imprinted nanostructures with high surface-to-volume ratio can further increase the amount of the imprinted sites in the proximity of the surface. It has clearly been shown that the combination of surface assembly imprinting with nanostructures can more significantly improve the binding capacity and binding kinetics than the only use of porogens in traditional approaches. In particular, tubular nanostructure is the most favorable for improving the molecular recognition properties of imprinted materials. The imprinted nanowires and nanotubes should be desirable forms to meet the requirements for applications as recognition components of nanosensors and could potentially be exploited in detecting the highly explosive and environmentally deleterious chemicals.

ACKNOWLEDGMENT

This work was supported by National Natural Science Foundation of China (60571038, 90406024) and National Basic Research Program of China (2006CB300407). We also thank the Centurial Program of the Chinese Academy of Sciences for the financial support and acknowledge the innovation project of Chinese Academy of Sciences.

Received for review August 13, 2006. Accepted October 5, 2006.

AC0615044